BENDING STRENGTH OF CROSS LAMINATED TIMBER BEAMS LOADED IN PLANE

Marcus Flaig[1], Hans Joachim Blaß[2]

ABSTRACT: A computer aided numerical model for the simulation of the in-plane bending strength of CLT beams is presented. The model uses the Monte-Carlo-Method to generate mechanical characteristics of board lamellae and is suitable for the investigation of statistical effects such as homogenisation and size effects. Six different types of CLT beams, varying in size and in layup, were tested to validate the model and except for beams with only one lamella in direction of the beam height good agreement was found between the experimental results and the model's simulations.

KEYWORDS: cross laminated timber, beam, in-plane bending strength, homogenisation, size-effect

1 INTRODUCTION

Today, the range of applications of CLT products mainly covers planar components, such as wall, floor or roof elements. But the material is also suitable for beam type members and, moreover, due to transversal layers CLT is less susceptible to cracks than other solid timber materials such as glulam. But the transversal layers which are an integral part of the material do not contribute to the bending strength of CLT beams. Nonetheless, the results of numerous tests with CLT beams have shown that the reduction of the load-bearing cross-sectional area due to transversal layers is compensated by an increased in-plane bending strength compared to glulam made of equivalent lamellae. The high bending strength of CLT beams is mainly due to homogenisation effects resulting from the parallel arrangement of multiple longitudinal lamellae at the most stressed edges of a cross section. In addition, the transversal layers, although reducing the cross section, also positively influence the bending strength by impeding the progression of cracks in longitudinal lamellae.
The comprehensive description of homogenisation effects in CLT beams, which are of statistical nature, requires extensive data on the bending strength of CLT beams that either can be obtained through experimental investigations, or by means of numerical simulations. The latter, in addition to much lower costs, offers the possibility to investigate statistical effects on a broad scale.

2 COMPUTATIONAL MODEL

2.1 GENERAL

Since CLT is composed of the same lamellae as glulam, major parts of an existing glulam model could be used for the numerical simulation of the bending strength of CLT beams. The employed glulam model, presented by Frese (2008) and based on the work of Colling (1990) and Görlacher (1990), consists of two major parts: a material model and a structural model.

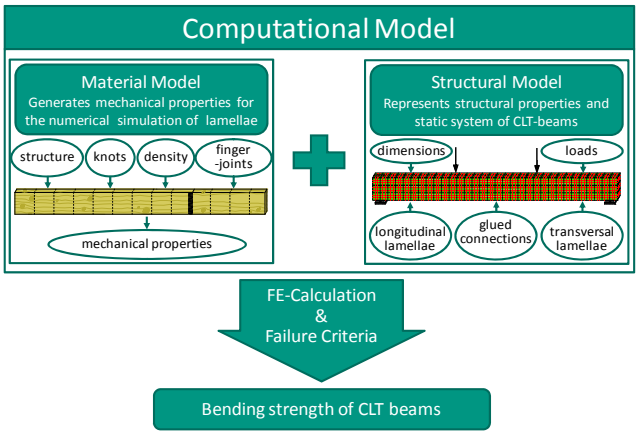

Figure 1: *Functional scheme of the computational model*

Both parts of the model have been adapted to the simulation of CLT beams. The material model, that so far in-

[1] Marcus Flaig, Karlsruhe Institute of Technology, Timber Structures and Building Construction, R.-Baumeister-Platz 1, 76131 Karlsruhe, Germany.
Email: marcus.flaig@kit.edu.
[2] Hans Joachim Blaß, Karlsruhe Institute of Technology, Timber Structures and Building Construction, R.-Baumeister-Platz 1, 76131 Karlsruhe, Germany.

cluded only algorithms to generate tensile and compressive strength and stiffness properties of boards and finger joints, was complemented with regression equations for the edgewise bending strength. The structural model, on the other hand, needed to be completely replaced due to the fundamentally different assembling of lamellae in glulam and in CLT, respectively.

2.2 PRICIPLE FUNCTIONING

The computational model takes into account not only the variation of mechanical properties between entire boards, but also accommodates the scatter within single boards. In the model, boards are divided into short sections with a length of 150 mm and individual mechanical properties are generated for each section. Like in real lamellae finger joints are interposed between subsequent boards. Strength and stiffness properties are calculated by means of regression equations using Monte-Carlo-Method and empirically obtained distribution functions of physical and morphological board characteristics, e.g. the density, the knot area ratio (KAR), the arrangement of knots and distance between finger joints.
The structural model represents the geometry of the simulated CLT beam and the test setup according to EN 408 by means of finite elements and is used to calculate bending stresses in longitudinal lamellae. Each lamella is modelled with beam elements and connected to transverse lamellae in the intersections by means of springs. Beam elements representing longitudinal lamellae have a consistent length of 150 mm to meet the conditions of the material model and each element can be assigned the strength and stiffness properties generated in the material model. Three spring elements connecting longitudinal and transversal beam elements in each intersection represent the stiffness of crossing areas between orthogonally bonded lamellae and permit the corresponding mutual displacements and rotations (cf. Figure 2). In the model the spring constants were calculated with a constant slip modulus of 5 N/mm³.

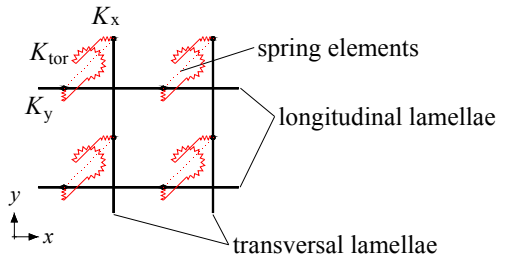

Figure 2: *Interconnection between longitudinal and transversal lamellae*

To determine the bending strength of simulated CLT beams, loads are applied in the third points of the span and increased stepwise. After every load step bending stresses in longitudinal lamellae are calculated from the internal forces of respective beam elements and for each section the stresses are compared to the strength properties generated in the material model. The failure of a board section or finger joint is identified by means of a stress based failure criterion F according to equation (1) assuming a linear interaction of stresses resulting from bending moments and normal forces. If the failure criterion reaches the value 1, the stiffness of the corresponding beam element is severely reduced and the element remains nearly stress free in subsequent load steps.

$$F_i = \frac{\sigma_{t,0,i}}{f_{t,0,i}} + \frac{\sigma_{m,i}}{f_{m,i}} \quad (1)$$

Then, the load is further increased until the next section fails and the procedure is repeated until either the beam collapses or a predefined abort criterion, e.g. the global deflection, is met. Subsequently, the bending strength of the simulated beam is calculated from the maximum load that has been applied during the whole process.

2.3 INPUT DATA

Input data modelling is the most essential component of the numerical simulation. Therefore, the basic components of the material model, i.e. distribution functions and regression equations that describe the properties of boards and finger joints, need to be derived from representative samples. The distribution functions and regression equations adopted from the glulam model are based on several thousand data sets and meet this requirement. An overview of the parameters taken from the glulam model is given in Table 1. A more detailed description can be found in Frese (2008).

Table 1: *Input data adopted from the glulam model*

Distribution functions	Regression equations
board length	MOE in tension
proportion of sections with knots	tensile strength
knot area ratio	MOE in compression
density	compressive strength

In contrast to glulam beams where normal stresses are more or less constant throughout the thickness of individual lamellae normal stresses vary significantly within the width of lamellae of CLT beams loaded in plane. Therefore, the edgewise bending strength of boards and finger joints needed to be introduced to the model and since no adequate data was available, that would have allowed for the calculation of regression equations, the edgewise bending strength and the correlated board properties were determined by tests.

3 EXPERIMENTAL INVESTIGATIONS

3.1 GENERAL

The experimental investigations described below include bending tests with CLT beams and edgewise bending tests with individual boards and finger joints. The test series with CLT beams were performed in order to determine the in-plane bending strength depending on the number of

longitudinal layers and the number of lamellae in direction of the beam height. Test series 2-1 through 6-1 were intended to investigate homogenisation effects in beams with only one lamella in direction of the beam height where the lamellae are subjected to pure edgewise bending whereas test series 2-2 and 3-2 were designed to validate the failure criterion used in the computational model.

To determine the edgewise bending strength of boards at first, bending tests with single boards without cross layers were performed (cf. section 3.3), but the simulated bending strength of CLT beams obtained on the basis of the regression equation derived from these tests proved to be too low compared to experimental values.

To find out, if the cross layers of CLT beams have any positive effect on the edgewise bending strength of longitudinal lamellae a small test series comprising 29 boards with a cross layer glued on one side was performed (cf. section 3.4). The results showed that cross layers significantly increase the edgewise bending strength especially in boards with large knots. Therefore, a third and more extensive test series was performed to determine the edgewise bending strength of boards with cross layers and to derive a regression equation to be used in the numerical model (cf. section 3.5).

The specimens of all test series described below were made from Norway spruce (Picea abies) with a mean moisture content of 10±1%. The material samples consisted of ungraded boards. For the bonding of CLT beams a two-component melamine-formaldehyde adhesive (MUF) was used.

3.2 TESTS WITH CLT-BEAMS

3.2.1 Material and methods

A total of sixty CLT beams were tested in six series, each comprising ten specimens, to determine the in-plane bending strength of CLT beams. Figure 3 shows the cross sections of the tested CLT beams.

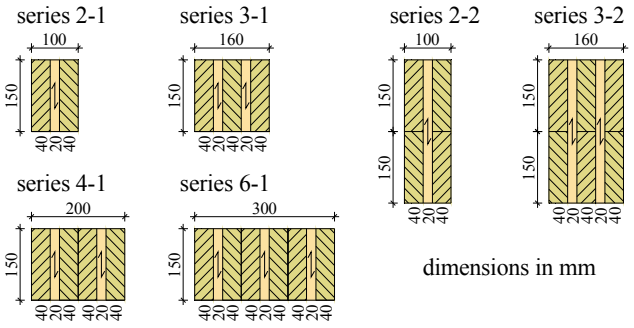

Figure 3: *Cross sections of tested CLT beams*

Before the manufacturing of the CLT slabs and the subsequent cutting of the test specimens from these, the density and the dynamic MOE of all longitudinal lamellae were measured. For a major part of the lamellae also the dimensions of knots within 150 mm long sections were recorded. This allowed for the determination of knot based visual grading parameters and the KAR-value which is used in the simulation program. The dynamic MOE was used to subdivide the boards into two classes of equal size.

Class 1: $E_{dyn} \geq 11{,}550$ N/mm², $\rho_{mean} = 455$ kg/m³

Class 2: $E_{dyn} < 11{,}550$ N/mm², $\rho_{mean} = 407$ kg/m³

Based on the knot measurements the lamellae were also visually graded according to German standard DIN 4074 (board grading) and assigned to the strength classes given in EN 338 in accordance with EN 1912.

Table 2: *Results of visual strength grading*

Board Class	Grading / strength class		
	S7 / C16	S10 / C24	S13 / C30
1	2%	39%	59%
2	19%	65%	16%

The bending tests to determine the in-plane bending strength and the MOE of the CLT beams were carried out according to EN 408. The specimens had a span of 18 times the beam height and two single loads were applied in third points. The local deflection between the load application points was measured in the neutral axis to determine the MOE. The complete setup is shown in Figure 4.

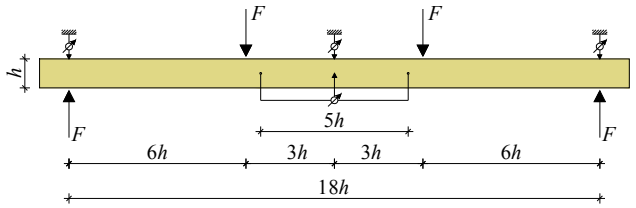

Figure 4: *Test setup to determine the bending strength of CLT beams and boards*

3.2.2 Results

In 59 of 60 specimens failure was caused by bending stresses. One specimen from series 2-2 failed due to shear stresses in the crossing areas. The failure rate in finger joints was 21% in specimens consisting of boards of class 1 whereas in specimens of class 2 only 7% of fractures occurred in finger joints. For each specimen the bending strength related to the net cross section of longitudinal layers was calculated from the maximum load. The 5th-percentiles of the bending strength were estimated for each test series assuming log-normal distributed values. The MOE related to the net cross section of longitudinal layers was evaluated from the load-slip curves between 10% and 40% of the maximum load. In Table 3 the results of all test series are given.

3.2.3 Discussion

Despite the relatively small size of the test series the increase of the 5th percentiles of bending strength and the decrease of the variation with increasing number of longitudinal layers is visible, but it is hardly possible to deduce reliable system strength factors from the values on hand and to describe the effect of homogenisation by means of a

parametric equation. The test results, however, are not in contradiction to the results of numerical simulations, as will be shown later.

The low percentage of failures in finger joints indicates that the average edgewise bending strength of these connections is higher than the average edgewise bending strength of weak board sections. The presumption is confirmed by the results of the bending tests with boards and finger joints described below.

Table 3: *Bending strength and MOE of tested CLT beams*

Board class	Series	Number of specimens	$f_{m,net}$ in N/mm²			E_{net} in N/mm²
			MEAN	*STD*	*P5*	*MEAN*
1	2-1	6	41.6	7.16	31.2	12683
	3-1	6	46.4	6.26	36.7	12835
	4-1	5	41.5	4.63	34.5	13118
	6-1	5	46.2	5.27	37.8	12830
	2-2	5	45.0	9.63	29.0	15072
	3-2	5	37.5	2.89	33.0	12856
2	2-1	4	38.5	12.7	20.1	9878
	3-1	4	36.0	3.90	30.0	11430
	4-1	5	39.0	4.12	32.6	11156
	6-1	5	36.5	4.40	29.9	10260
	2-2	5	26.4	6.04	18.5	9976
	3-2	5	27.8	3.91	21.9	9654

MEAN mean value, *STD* standard deviation, *P5* 5th percentile

3.3 BOARDS WITHOUT CROSS LAYER

3.3.1 Material and methods

Bending tests according to EN 408 with the test setup shown in Figure 4 were performed to determine the edgewise bending strength of boards used for the production of CLT. 102 boards with a thickness of 40 mm and a width of 150 mm were tested. Before the tests the board density, the dynamic MOE and the dimensions of knots were determined. In Figure 5 the frequency distributions of the board density and the knot area ratio of board sections where failure occurred are given.

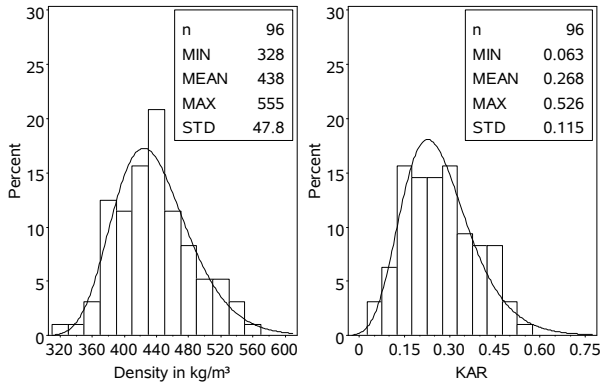

Figure 5: *Density and KAR-values of tested boards without cross layer*

3.3.2 Results

96 of 102 boards failed due to bending stresses, in the remaining six boards failure was caused by shear stresses. In 93 boards fracture started in the tension zone. Only three boards showed compressive wrinkles before the ultimate load was reached. From the ultimate load and the measured deflection the bending strength and the MOE were determined for each specimen. Figure 6 shows the obtained frequency distributions of both characteristics. The obtained data was used to calculate regression equations (2) and (3) by means of multiple regression analyses.

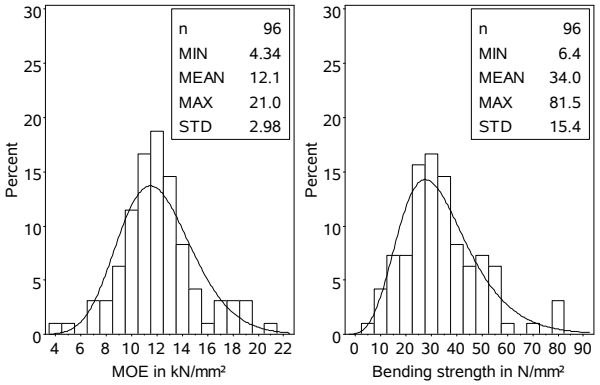

Figure 6: *MOE and bending strength of tested boards without cross layer*

$$\ln(E_m) = 7.90 + 3.81 \cdot 10^{-3} \cdot \rho_0 - 0.369 \cdot KAR$$
$$r = 0.773 \qquad s_R = 0.165 \qquad (2)$$
$$\text{mit } E_m \text{ in N/mm}^2;\ \rho_0 \text{ in kg/m}^3$$

$$\ln(f_m) = -9.09 + 1.36 \cdot \ln(E_m) - 0.978 \cdot KAR$$
$$r = 0,839 \qquad s_R = 0,274 \qquad (3)$$
$$\text{mit } f_m \text{ in N/mm}^2;\ E_m \text{ in N/mm}^2$$

Using the recorded knot measurements the boards were visually graded according to German standard DIN 4074 and assigned to the strength classes given in EN 338. In Table 4 the results are given for the three grading and strength classes covered by the tested sample.

Table 4: *Test results by strength class*

Grading / strength class	Number of specimens	ρ_u in kg/m³	E_{net} in N/mm²	*KAR*	$f_{m,mean}$ in N/mm²	$f_{m,05}$ in N/mm²
		MEAN	*MEAN*	*MEAN*	*MEAN*	*P5*
S7 / C16	18	408	10211	0.414	21.2	7.7
S10 / C24	48	428	11568	0.265	32.5	15.8
S13 / C30	30	471	14119	0.184	44.1	22.1

MEAN mean value, *P5* 5th percentile

3.3.3 Discussion

The test results given in Table 4 clearly show that the experimentally obtained 5th percentiles of the bending

strength are significantly lower than the characteristic bending strengths of the corresponding C-classes given in European standard EN 338. This is not surprising, since the criteria given in DIN 4074 that were used for the visual grading of the tested boards are based on tension tests and therefore do not allow for a classification into strength classes referring to the bending strength. This problem, of course, only affects countries where DIN 4074 is applied for strength grading.
Nonetheless, the test results demonstrate the large difference between the edgewise bending strength of boards and the bending strength of CLT beams and thereby indicate the strong effect of homogenisation occurring in CLT beams.

3.4 BOARDS WITH CROSS LAYER - PRELIMINARY TESTS

3.4.1 Material and methods

The test material consisted of 29 boards with a width of 150 mm and a thickness of 35 mm. The boards were cut from longitudinal layers of CLT slabs in such a way that a cross layer with a thickness of 5 mm remained on one side resulting in a total thickness of the specimens of 40 mm.

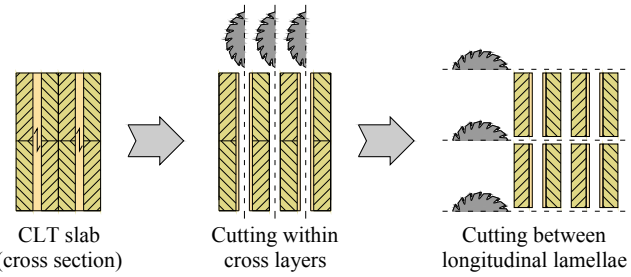

Figure 7: *Cutting of boards with cross layers from CLT slabs*

The density, the dynamic MOE and the measurements of knots on the three visible surfaces of the boards were determined before testing. After testing the cross layers were removed to measure knots on the hidden surface. In Figure 8 the frequency distributions of the board density and the knot area ratio of board sections where failure occurred are given.

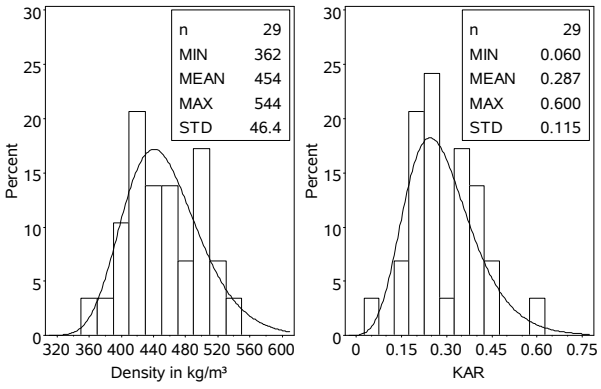

Figure 8: *Density and KAR-values of tested boards with cross layer (preliminary test series)*

3.4.2 Results

In all 29 boards failure was caused by bending stresses in the tension zone. The frequency distributions of bending strength and the MOE calculated from the test results are given in Figure 9.

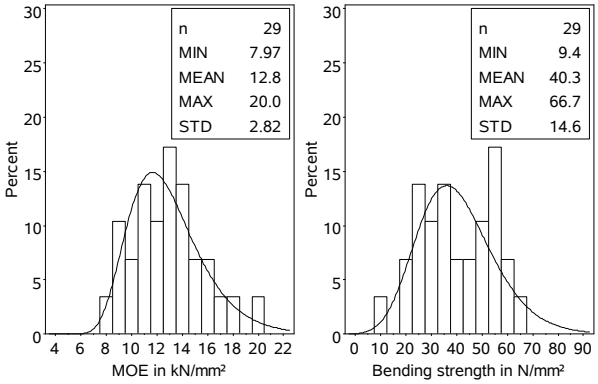

Figure 9: *MOE and bending strength of tested boards with cross layer (preliminary test series)*

3.4.3 Discussion

Density, KAR and MOE of the tested board samples with and without cross layers show good agreement in extreme and average values. Two-sample Kolmogorov-Smirnov tests also revealed no significant differences in the empirical distribution functions at a level of 0.05, so that the two tested samples can be considered equivalent both objectively and in statistical terms. Figure 10 shows the bending strength obtained from both test series plotted against MOE and KAR-values and the regression lines determined separately for each sample.

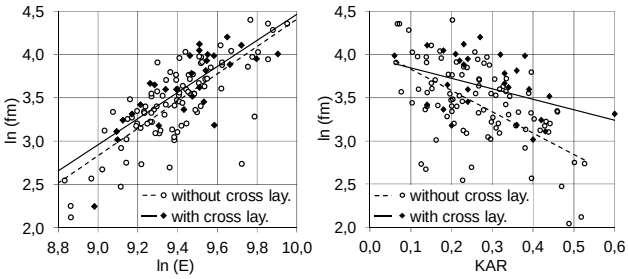

Figure 10: *Edgewise bending strength of softwood boards with and without cross layer plotted against ln(E) and KAR*

The distance between the two regression lines in the left diagram shows that on average the bending strength of boards with cross layers is higher than for boards without cross layers. The influence of the MOE, however, is scarcely influenced by cross layers resulting in regression lines with almost identical slope. The cause of the upward shift of the regression line for boards with cross layers can be seen in the diagram on the right side. Here, the different slopes of the two regression lines show that in boards with cross layers the influence of knots is significantly smaller than in boards without cross layer which results in the observed higher mean bending strength of boards with cross layers.

Since the bending strength of boards with large knots is usually rather small this effect is even stronger on the level of 5th percentiles.

3.5 BOARDS WITH CROSS LAYER - WITHIN MEMBER VARIABILITY

3.5.1 Material and methods

The test material to determine the bending strength of boards with cross layers consisted of 66 boards with a cross section of 140 x 33 mm². As in the preliminary test series the boards were cut from CLT slabs and a cross layer with a thickness of 7 mm was left on one side resulting in a total thickness of the specimens of 40 mm. For the numerical simulation it is important not only to know the overall variability of the bending strength but also the variability within individual boards. To determine the within and the between member variability several "weak" sections were tested within each board so that the residuals resulting from a subsequent regression analysis could be divided into two respective parts. The "weak" sections to be tested were identified by means of knots and cut from the boards with a length of 1 m. The number of test sections obtained from individual boards varied between two and four resulting in a total of 154 test sections. Again the density and the knot measurements were determined before testing.

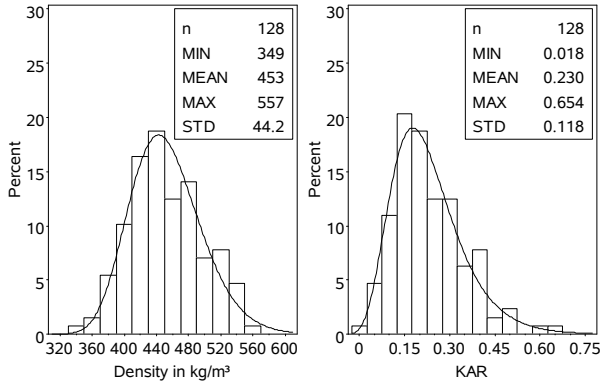

Figure 11: *Density and KAR-values of tested boards with cross layer (main test series)*

To determine the bending strength four point bending tests with a reduced span of twelve times the board width were performed. To obtain a sufficient length the test sections were extended at both ends by LVL-strips connected with finger joints.

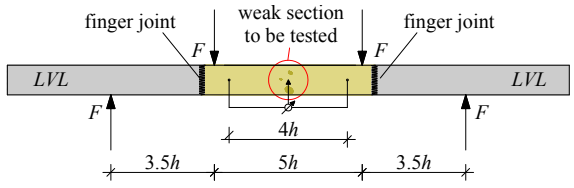

Figure 12: *Test setup to determine the bending strength of boards with cross layer (main test series)*

3.5.2 Results

In 46 specimens (30%) failure occurred in finger joints. The bending strength obtained from these specimens varied between 19.1 and 60.0 N/mm² with a mean value of 44.8 N/mm² whereas the bending strength of specimens that failed between the finger joints varied between 7.0 and 62.2 N/mm² with a mean value of 38.2 N/mm².

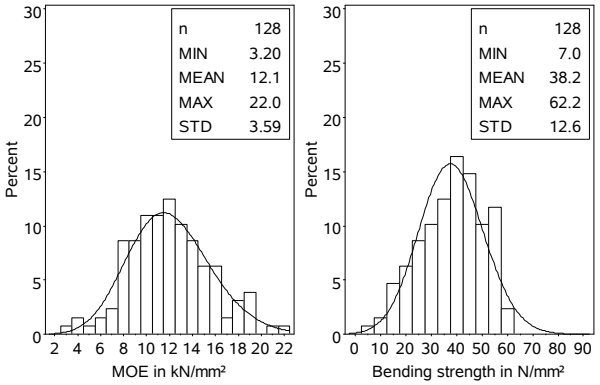

Figure 13: *MOE and bending strength of tested boards with cross layer (main test series)*

To ensure that high bending strengths are adequately represented by the regression equations specimens that failed in finger joints were considered in the regression analyses if the bending strength was higher than 45 N/mm². Altogether, the data of 128 tested board sections were used to calculate regression equations (4) and (5).

$$\ln(E_m) = 8.11 + 3.50 \cdot 10^{-3} \cdot \rho_0 - 0.608 \cdot KAR$$
$$r = 0.739 \qquad s_R = 0.186 \qquad (4)$$
$$E_m \text{ in } \mathrm{N/mm^2};\ \rho_0 \text{ in } \mathrm{kg/m^3}$$

$$\ln(f_m) = -4.97 + 0.935 \cdot \ln(E_m) - 0.687 \cdot KAR$$
$$r = 0.776 \qquad s_R = 0.240 \qquad (5)$$
$$f_m,\ E_m \text{ in } \mathrm{N/mm^2}$$

In Figure 13 the logarithmised values of MOE and bending strength obtained from the tests are plotted against the predicted values calculated according equations (4) and (5).

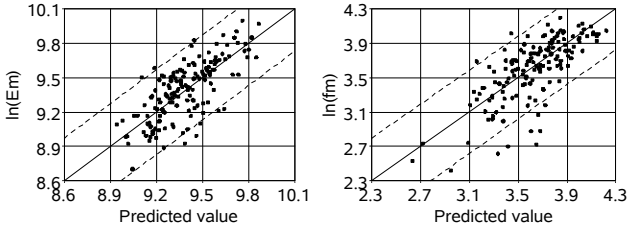

Figure 14: *Actual vs. predicted values of MOE and bending strength of boards with cross layers*

The standard deviations s_R given in equations (4) and (5) describe the overall variation of MOE and bending strength. The within member variability $s_{R,B}$ and the between member

variability Δ_B resulting from residual analyses are given in equations (6) and (7).

$$\ln(E_m): \; s_{R,B} \sim N(0, 0.1097) \quad \Delta_{R,B} \sim N(0, 0.1498) \qquad (6)$$

$$\ln(f_m): \; s_{R,B} \sim N(0, 0.1709) \quad \Delta_{R,B} \sim N(0, 0.1690) \qquad (7)$$

3.5.3 Discussion

Although the tested sample covers a wide range of material properties, board sections with high bending strength are underrepresented by the regression equations, first of all because only "weak" sections were chosen for testing but also because the better ones of the tested "weak" sections did not fail. For the numerical simulation, however, the accurate description of weak sections is most important since the strength of a board is always governed by these sections.

3.6 TESTS WITH FINGER JOINTS

3.6.1 Material and methods

To determine a regression equation for the edgewise bending strength of finger joints bending tests with finger jointed boards were performed. The test material consisted of 362 softwood lamellae, each composed of two boards connected by finger joints in the middle of the length. The test material was provided by five German CLT producers who use different finger joint profiles and orientations. Specimens of test series A to D were finger jointed flat wise, i.e. in such a way that the fingers were visible in flat sides, whereas in specimens of series E fingers were visible in edge sides. In order to determine a possible influence of the board width on the edgewise bending strength of finger joints, lamellae with four different widths were tested. Table 5 gives an overview on the different finger joint profiles and the dimensions of specimens.

Four point bending tests as illustrated in Figure 15 were performed to determine the edgewise bending strength of the finger jointed connections. In the test setup the distance between the two single loads was kept small to minimize the risk of failure apart from finger joints. As a consequence local deflections between the load application points were too small to be measured. Instead, the global deflection in the load application points and the vertical displacements at the supports were measured to determine the MOE of the specimens.

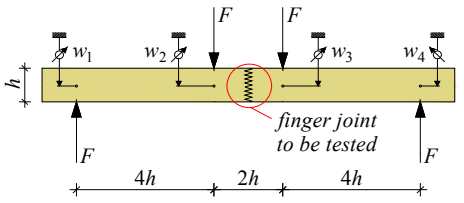

Figure 15: *Test setup to determine the bending strength of finger joints*

Table 5: *Finger joint profiles and board dimensions*

Producer	finger joint profile ℓ_{fj} / t_{fj} / b_{fj} / s	boards d / b	Number of specimens
A	20 / 6.2 / 1.0 / f	40/100	24
		40/150	20
		40/200	20
B	15 / 3.8 / 0.42 / f	40/100	20
		40/150	20
		33/250	20
C	20 / 6.2 / 1.0 / f	30/100	22
		30/200	22
		30/250	22
D	15 / 3.8 / 0.54 / f	30/150	20
		30/200	20
		30/250	19
E	15 / 3.8 / 0.3 / e	17/143	19
		17/195	18
		27/143	20
		27/195	20
		33/143	19
		33/195	17

ℓ_{fj} finger length, t_{fj} pitch, b_{fj} tip width, s orientation of finger joints (*f* flatwise, *e* edgewise), d board thickness, b board width

After performing the bending tests the densities of the boards on both sides of the finger joints were determined. In Figure ***16*** the frequency distributions of the minimum and the maximum board density in a connection are given.

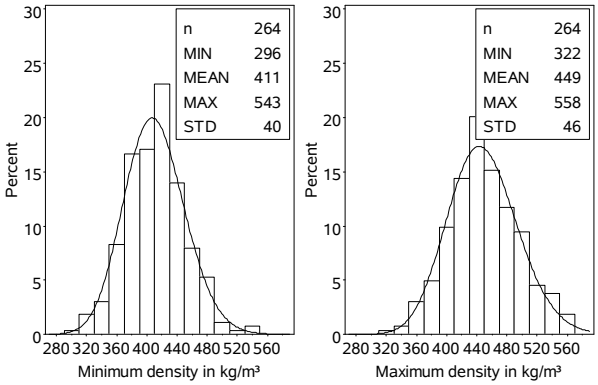

Figure 16: *Minimum and maximum board density of tested finger joints*

3.6.2 Results

In 264 specimens failure occurred in or emanated from the finger joint. 98 specimens failed apart from finger joints, mostly due to shear stresses. The bending strength and the MOE calculated from the test results are given in Figure 17. Since the local deflection could not be measured the MOE was evaluated from the global deformation. In the evaluation the proportion of bending deformation was calculated by subtracting the shear deformation, which was calculated with a shear modulus of 650 N/mm², and the displacement at the supports from the measured global deflection.

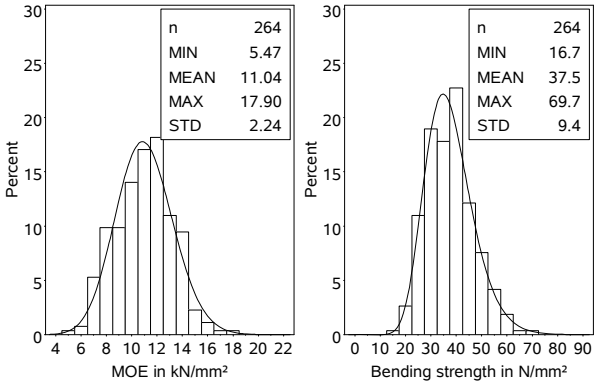

Figure 17: *MOE and bending strength of tested finger joints*

Regression equations (8) and (9) were derived from multiple regression analyses. In Figure 18 the measured values are plotted against the values calculated by the respective regression equation.

$$\ln(E_{m,j}) = 7.69 + 1.56 \cdot 10^{-3} \cdot \rho_{0,max} + 2.44 \cdot 10^{-3} \cdot \rho_{0,min}$$
$$r = 0.717 \qquad s_R = 0.149 \qquad (8)$$
$$E_{m,j} \text{ in } N/mm^2;\ \rho_{0,max}, \rho_{0,min} \text{ in } kg/m^3$$

$$\ln(f_{m,j}) = -3.93 + 0.813 \cdot \ln(E_{m,j}) - 1.56 \cdot 10^{-3} \cdot (h - 150)$$
$$r = 0.640 \qquad s_R = 0.195 \qquad (9)$$
$$\text{mit } f_{m,j},\ E_{m,j} \text{ in } N/mm^2;\ h \text{ in mm}$$

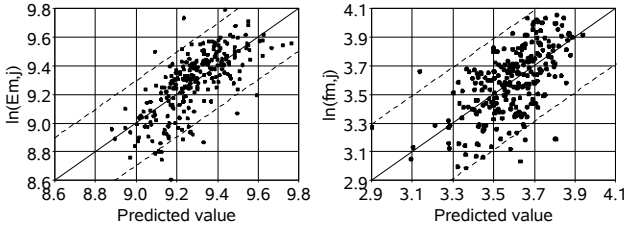

Figure 18: *Actual vs. predicted values of MOE and bending strength of finger joints in board lamellae*

3.6.3 Discussion

The comparison of the edgewise bending strength of finger joints with the edgewise bending strength of boards with cross layers shows that both distributions have similar mean values but the minimum values differ significantly. The absence of values below 16.7 N/mm² for finger joints explains the relatively low percentages of failures in finger joints that were observed in tests with CLT beams.

4 NUMERICAL SIMULATION

4.1 GENERAL

In a first series of simulations the tests described in section 3.2 were reproduced. For these simulations distribution functions of the board density and the KAR-value were derived from the recorded test data and used as input data. The aim of these simulations was to validate the newly implemented parts of the computational model, in particular, the regression equations for the edgewise bending strength and the linear interaction of tensile stresses and bending stresses used as failure criterion in the tension zone.

In a further series of simulations the bending strength of beams with a height of 600 mm was determined to be able to compare the bending strength of CLT beams and glulam beams. In these simulations the material properties for visually graded boards of grading class S10 were used which result in beams of strength class GL24h when used for the production of glulam beams. To investigate the influence of the beam layup on the bending strength of CLT beams the number of longitudinal layers n and the number of lamellae within longitudinal layers m was varied within the series

A third series of simulations was performed to study size effects in CLT beams. In four sub-series two different layups, one with two and another with four longitudinal layers, and longitudinal lamellae of two different widths, 100 mm and 150 mm, were considered. Within each sub-series the width of longitudinal lamellae was kept constant whereas the number of lamellae in longitudinal layers varied between four and twelve, i.e. the beam height was increased by increasing the number of lamellae in longitudinal layers. In all sub-series again the material properties for visually graded boards of grading class S10 were used.

4.2 SIMULATION RESULTS

The results of the performed simulations are given in Table 6 to Table 9 below. All bending strengths given in the tables are related to the net thickness of longitudinal layers and expressed in N/mm². Each value represents 1000 simulated beams with a span of 18 times the beam height.

In Table 6 and Table 7 the results of the first series of simulations and the results of the respective test series are summarized. The simulated bending strength $f_{m,05,sim}$ and system strength factors k_{sys}, calculated as the ratio of the bending strength of the considered beam type and the bending strength of a single board are quoted. In the lower part of the tables the values derived from tests are opposed. The given characteristic values $f_{m,k,EN}$ were calculated according to EN 14358 whereas the 5th percentiles $f_{m,05,log}$ and the upper (UCL) and lower (LCL) 95%-limits of a two-sided confidence interval were estimated on the assumption of lognormal distributed values.

Considering the small size of the tested samples the agreement between the simulated and the experimentally obtained characteristic bending strength is fairly good for single boards (series 1-1) and for beams with two lamellae per longitudinal layer (series 2-2 and 3-2). For beams with one lamella in direction of the height (series 2-1 to 6-1) the strong homogenisation that is observed in the test results cannot be reproduced by the model and the characteristic bending strengths obtained from simulations are significantly lower than the experimentally obtained values.

Table 6: *Simulated and experimentally obtained bending strength for CLT beams of class 1 ($E_{dyn} \geq 11550$ N/mm²)*

	series	1-1	2-1	3-1	4-1	5-1	6-1	2-2	3-2
SIM	$f_{m,05,sim}$	23.1	24.1	24.9	25.3	25.4	25.7	27.4	28.2
	k_{sys}	1.00	1.05	1.08	1.10	1.10	1.11	1.19	1.22
TESTS	$f_{m,k,EN}$	26.0	27.5	33.2	31.5	-	34.3	23.6	31.0
	$f_{m,05,log}$	26.3	31.2	36.7	34.5	-	37.8	29.0	33.0
	LCL	25.9	19.7	25.3	23.5	-	25.0	12.0	25.2
	UCL	30.6	36.2	41.5	38.3	-	42.3	37.0	35.5

k_{sys} system strength factor, *UCL/LCL* 95% confidence limits

Table 7: *Simulated and experimentally obtained bending strength for CLT beams of class 2 ($E_{dyn} < 11550$ N/mm²)*

	series	1-1	2-1	3-1	4-1	5-1	6-1	2-2	3-2
SIM	$f_{m,05,sim}$	17.6	18.6	19.2	19.6	19.6	19.9	21.1	21.6
	k_{sys}	1.00	1.06	1.09	1.11	1.12	1.13	1.20	1.23
TESTS	$f_{m,k,EN}$	15.1	13.1	26.5	29.9	-	27.2	15.7	19.6
	$f_{m,05,log}$	15.9	20.1	30.0	32.6	-	29.9	18.5	21.9
	LCL	13.4	3.2	17.6	22.6	-	19.9	9.1	13.5
	UCL	18.0	29.4	33.6	36.1	-	33.5	22.5	25.0

k_{sys} system strength factor, *UCL/LCL* 95% confidence limits

In Table 8 the 5th percentiles of the bending strength obtained from the second series of simulations are given. The curves and values clearly show that the bending strength of CLT beams not only depends on the number n of longitudinal layers in a cross section but also on the number m of lamellae within longitudinal layers. The comparison of the values with the characteristic strength properties of the boards, 15.8 N/mm² in bending and 14 N/mm² in tension, reveals the strong homogenisation occurring in CLT beams. The resulting bending strengths of CLT beams are 8% to 32% higher than the characteristic bending strength of glulam beams composed of lamellae of the same strength class.

Table 8: *Simulated bending strength $f_{m,05,sim}$ of CLT beams with a height of 600 mm*

n	2	3	4	5	6
$m = 4$	25.8	27.0	27.6	28.1	28.2
$m = 5$	26.5	28.2	28.8	29.2	29.8
$m = 6$	27.6	29.1	30.0	30.2	30.8
$m = 8$	29.1	30.2	30.8	31.6	31.7

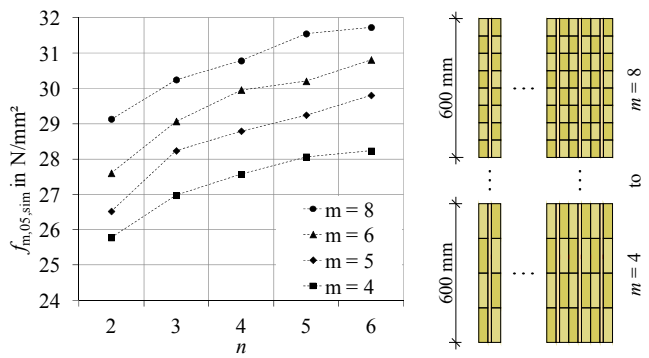

m = number of lamellae per longitudinal layer
n = number of longitudinal layers

$n = 2$ to $n = 6$

The results of the third series of simulations are quoted in Table 9. For the calculation of the size factors k_h for the different beam types the bending strengths of beams with a height of 600 mm were chosen as reference values.
Starting from the reference beams the bending strength at first rises with increasing beam height. This effect is due to the homogenisation in direction of the beam height which for the considered beams results in an increase of the bending strength that is greater than the loss due to the larger size. In the diagrams given in Table 9 the size factors for CLT beams are plotted against the beam height and the number of lamellae in longitudinal layers. For comparison the size factors for glulam beams that were derived from the results of numerical simulations by Frese (2008) are given in the upper diagram.

Table 9: *Simulated 5th percentiles of bending strength and size factors for selective CLT beams*

$n = 4$, $b_L = 150$ mm									
h	600	750	900	1050	1200	1350	1500	1650	1800
$f_{m,05,sim}$	27.6	28.4	29.2	29.4	29.5	29.3	28.9	28.5	28.3
k_h	1.00	1.03	1.06	1.07	1.07	1.06	1.05	1.03	1.02
$n = 2$, $b_L = 150$ mm									
h	600	750	900	1050	1200	1350	1500	1650	1800
$f_{m,05,sim}$	25.8	26.6	27.2	27.6	27.4	27.3	27.5	27.1	26.7
k_h	1.00	1.03	1.06	1.07	1.06	1.06	1.07	1.05	1.04
$n = 4$, $b_L = 100$ mm									
h	400	500	600	700	800	900	1000	1100	1200
$f_{m,05,sim}$	26.2	26.9	27.9	28.4	28.8	28.8	28.8	28.6	28.3
k_h	0.94	0.96	1.00	1.02	1.03	1.03	1.03	1.02	1.01
$n = 2$, $b_L = 100$ mm									
h	400	500	600	700	800	900	1000	1100	1200
$f_{m,05,sim}$	27.8	28.6	29.8	30.1	30.5	30.7	30.8	30.4	30.1
k_h	0.94	0.96	1.00	1.01	1.03	1.03	1.04	1.02	1.01

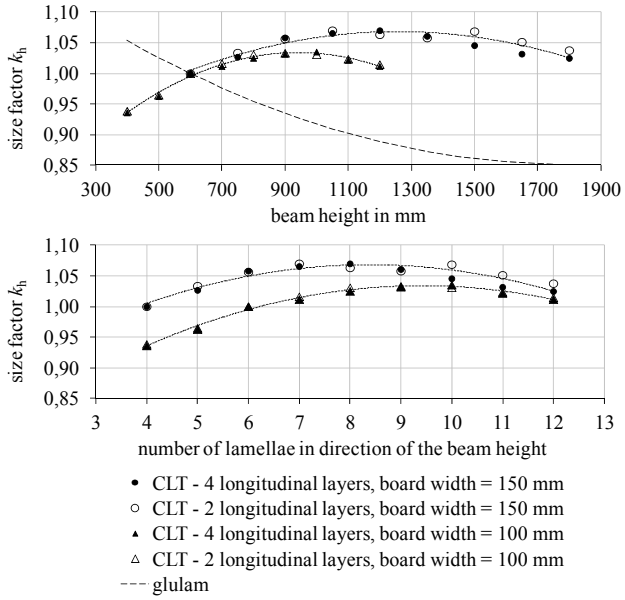

n number of longitudinal layers, h beam height in mm,
b_L width of longitudinal lamellae , k_h size factor

5 SUMMARY AND CONCLUSIONS

A computational model for the numerical simulation of the in-plane bending strength of CLT beams that was developed on the basis of an established model for the numerical simulation of glulam beams is presented and essential modifications and supplementations with respect to the original model are described.

By means of the model it has been shown that the bending strength of CLT beams strongly depends on the number of lamellae within both the thickness and the height of a cross section. The results obtained from the numerical model so far indicate that the bending strength of CLT beams is considerably higher than for glulam composed of lamellae of the same strength class. Moreover, the strong homogenisation in direction of the height of CLT beams results in a reversed size effect, i.e. an increase of the bending strength with increasing beam height.

While the simulated bending strength of relatively small CLT beams with a height of 300 mm has already been confirmed by tests, the respective values for larger beams are still to be validated by further tests, especially with beams with a reference height of 600 mm.

REFERENCES

[1] Blaß, H. J.; Frese, M.; Glos, P.; Denzler, J.; Linsenmann, P.; Ranta-Maunus, A.: Zuverlässigkeit von Fichten-Brettschichtholz mit modifiziertem Aufbau. Universität Karlsruhe (TH), 2008.

[2] Colling F.: Tragfähigkeit von Biegeträgern aus Brettschichtholz in Abhängigkeit von den festigkeitsrelevanten Einflussgrößen. Dissertation, Universität Karlsruhe (TH), 1990.

[3] Faye C., Rouger F., Garcia P.: Experimental investigations on mechanical behavior of glued solid timber. In: *Proceedings. CIB-W18 Meeting 43*, Paper 43-12-4. Nelson, New Zealand, 2010.

[4] Flaig, M: Biegeträger aus Brettsperrholz bei Beanspruchung in Plattenebene. Dissertation, Karlsruhe Institute of Technology, KIT Scientific Publishing, Karlsruhe, Germany, 2013.

[5] Foschi R.O., Barrett J.D.: Glued laminated beam strength: a model. In: *Journal of the structural division ASCE*, Vol. 106, No. ST8, 1735 - 1754, 1980.

[6] Görlacher R.: Klassifizierung von Brettschichtholzlamellen durch Longitudinalschwingungen. Dissertation, Universität Karlsruhe (TH), 1990.

[7] Isaksson T. (1999): Modelling the Variability of Bending Strength in Structural Timber. Report TVBK-1015, Dissertation, Department of Structural Engineering, Lund University, Sweden, 1999.

[8] Isaksson T., Thelandersson S., Moller-Pedersen T.: Within member variability of bending strength of timber. In: *Proceedings. PTEC Pacific Timber Engineering Conference*, Gold Coast, Australia, 1994.

[9] Källsner B., Salmela K., Ditlevsen, O.: A weak zone model for timber in bending. In: *Proceedings. CIB-W18 Meeting 30*, Paper 30-10-3, Vancouver, Canada, 1997.